Test of Lorentz and CPT violation with short baseline neutrino oscillation excesses

MiniBooNE Collaboration

A.A. Aguilar-Arevalo [n], C.E. Anderson [s], A.O. Bazarko [p], S.J. Brice [h], B.C. Brown [h], L. Bugel [m], J. Cao [o], L. Coney [f,1], J.M. Conrad [m], D.C. Cox [j], A. Curioni [s], R. Dharmapalan [a], Z. Djurcic [b], D.A. Finley [h], B.T. Fleming [s], R. Ford [h], F.G. Garcia [h], G.T. Garvey [k], J. Grange [i], C. Green [h,k], J.A. Green [j,k], T.L. Hart [e], E. Hawker [d,k], W. Huelsnitz [k], R. Imlay [l], R.A. Johnson [d], G. Karagiorgi [m], P. Kasper [h], T. Katori [j,m,*,2], T. Kobilarcik [h], I. Kourbanis [h], S. Koutsoliotas [c], E.M. Laird [p], S.K. Linden [s], J.M. Link [r], Y. Liu [o], Y. Liu [a], W.C. Louis [k], K.B.M. Mahn [f], W. Marsh [h], C. Mauger [k], V.T. McGary [m], G. McGregor [k], W. Metcalf [l], P.D. Meyers [p], F. Mills [h], G.B. Mills [k], J. Monroe [f], C.D. Moore [h], J. Mousseau [i], R.H. Nelson [e], P. Nienaber [q], J.A. Nowak [l], B. Osmanov [i], S. Ouedraogo [l], R.B. Patterson [p], Z. Pavlovic [k], D. Perevalov [a,h], C.C. Polly [h], E. Prebys [h], J.L. Raaf [d], H. Ray [i], B.P. Roe [o], A.D. Russell [h], V. Sandberg [k], R. Schirato [k], D. Schmitz [h], M.H. Shaevitz [f], F.C. Shoemaker [p,3], D. Smith [g], M. Soderberg [s], M. Sorel [f,4], P. Spentzouris [h], J. Spitz [s], I. Stancu [a], R.J. Stefanski [h], M. Sung [l], H.A. Tanaka [p], R. Tayloe [j], M. Tzanov [l], R.G. Van de Water [k], M.O. Wascko [l,5], D.H. White [k], M.J. Wilking [e], H.J. Yang [o], G.P. Zeller [h], E.D. Zimmerman [e]

[a] University of Alabama, Tuscaloosa, AL 35487, USA
[b] Argonne National Laboratory, Argonne, IL 60439, USA
[c] Bucknell University, Lewisburg, PA 17837, USA
[d] University of Cincinnati, Cincinnati, OH 45221, USA
[e] University of Colorado, Boulder, CO 80309, USA
[f] Columbia University, New York, NY 10027, USA
[g] Embry Riddle Aeronautical University, Prescott, AZ 86301, USA
[h] Fermi National Accelerator Laboratory, Batavia, IL 60510, USA
[i] University of Florida, Gainesville, FL 32611, USA
[j] Indiana University, Bloomington, IN 47405, USA
[k] Los Alamos National Laboratory, Los Alamos, NM 87545, USA
[l] Louisiana State University, Baton Rouge, LA 70803, USA
[m] Massachusetts Institute of Technology, Cambridge, MA 02139, USA
[n] Instituto de Ciencias Nucleares, Universidad Nacional Autónoma de México, D.F. 04510, Mexico
[o] University of Michigan, Ann Arbor, MI 48109, USA
[p] Princeton University, Princeton, NJ 08544, USA
[q] Saint Mary's University of Minnesota, Winona, MN 55987, USA
[r] Virginia Polytechnic Institute & State University, Blacksburg, VA 24061, USA
[s] Yale University, New Haven, CT 06520, USA

ARTICLE INFO

ABSTRACT

The sidereal time dependence of MiniBooNE ν_e and $\bar{\nu}_e$ appearance data is analyzed to search for evidence of Lorentz and CPT violation. An unbinned Kolmogorov–Smirnov (K–S) test shows both the ν_e and $\bar{\nu}_e$ appearance data are compatible with the null sidereal variation hypothesis to more than 5%. Using an unbinned likelihood fit with a Lorentz-violating oscillation model derived from the Standard Model Extension (SME) to describe any excess events over background, we find that the ν_e appearance data prefer a sidereal time-independent solution, and the $\bar{\nu}_e$ appearance data slightly prefer a sidereal time-dependent solution. Limits of order 10^{-20} GeV are placed on combinations of SME coefficients. These

* Corresponding author at: Massachusetts Institute of Technology, Cambridge, MA 02139, USA. Tel.: +1 630 840 4759; fax: +1 630 840 6520.
  E-mail address: katori@fnal.gov (T. Katori).

Neutrino oscillation
Lorentz violation

limits give the best limits on certain SME coefficients for $\nu_\mu \to \nu_e$ and $\bar\nu_\mu \to \bar\nu_e$ oscillations. The fit values and limits of combinations of SME coefficients are provided.

1. Introduction to Lorentz violation

Violation of Lorentz invariance and CPT symmetry is a predicted phenomenon of Planck-scale physics, especially with a spontaneous violation [1], and it does not require any modifications in quantum field theory or general relativity. Since neutrino oscillation experiments are natural interferometers, they can serve as sensitive probes of spacetime structure. Thus, neutrino oscillations have the potential to provide the first experimental evidence for Lorentz and CPT violation through evidence of oscillations that deviate from the standard L/E dependence [2], or that show sidereal time-dependent oscillations as a consequence of a preferred direction in the universe [3].

In this Letter, we test the MiniBooNE $\nu_\mu \to \nu_e$ and $\bar\nu_\mu \to \bar\nu_e$ oscillation data [4,5] for the presence of a Lorentz violation signal. Similar analyses have been performed in other oscillation experiments, including LSND [6], MINOS [7], and IceCube [8]. Naively, experiments with longer baselines and higher energy neutrinos would be expected to have better sensitivity to Lorentz violation because small Lorentz-violating terms are more prominent at high energy, where neutrino mass terms are negligible. However, some Lorentz-violating neutrino oscillation models mimic the standard massive neutrino oscillation energy dependence [9]. Then, in this case, the signal may only be seen in sidereal variations of oscillation experiments.

2. MiniBooNE experiment

MiniBooNE is a ν_e ($\bar\nu_e$) appearance short baseline neutrino oscillation experiment at Fermilab. Neutrinos are created by the Booster Neutrino Beamline (BNB), which produces a 93% (83%) pure ν_μ ($\bar\nu_\mu$) beam in neutrino (anti-neutrino) mode, determined by the polarity of the magnetic focusing horn. The MiniBooNE Cherenkov detector, a 12.2 m diameter sphere filled with mineral oil, is used to detect charged particles from neutrino interactions and is located 541 m from the neutrino production target. It is equipped with 1280 8 inch PMTs in an optically separated inner volume and 240 8 inch veto PMTs in an outer veto region. Details of the detector and the BNB can be found elsewhere [10,11]. Charged leptons created by neutrino interactions in the detector produce Cherenkov photons, which are used to reconstruct charged particle tracks [12]. The measured angle and kinetic energy of the charged leptons are used to reconstruct the neutrino energy, E_ν^{QE}, for each event, under the assumption that the target nucleon is at rest inside the nucleus and the interaction type is charged current quasielastic (CCQE) [13].

For this analysis, we use the background and error estimates from [14] (neutrino mode) and [15] (anti-neutrino mode). For neutrino mode, data from 6.46×10^{20} protons on target (POT) are used. An excess in the "low-energy" region ($200 < E_\nu^{QE}$(MeV) $<$ 475) was observed, with 544 events reported as compared to the prediction, 409.8 ± 23.3(stat.) ± 38.3(syst.). Interestingly, this excess does not show the expected L/E energy dependence of a

simple two massive neutrino oscillation model. Additionally, it is not consistent with the energy region expected for the "LSND" signal [16]. For the anti-neutrino mode analysis (5.66×10^{20} POT), MiniBooNE observed a small excess in the low-energy region, and an excess in the region $475 < E_\nu^{QE}$(MeV) < 1300. The excess in this "high-energy" region is found to be consistent with the LSND signal, assuming a two massive neutrino hypothesis, but remains statistically marginal. In the "combined" region ($200 < E_\nu^{QE}$(MeV) $<$ 1300), MiniBooNE observed 241 $\bar\nu_e$ candidate events as compared to the prediction, 200.7 ± 15.5(stat.) ± 14.3(syst.).

Although the conflict between MiniBooNE neutrino and anti-neutrino mode results can be resolved in models without CPT violation [17], CPT violation is a viable option. Since CPT violation necessarily implies violation of Lorentz invariance within interactive quantum field theory [18], we are in a well-motivated position to search for Lorentz and CPT violation using the MiniBooNE data. In fact, proposed models motivated by Lorentz violation [19,20] can already accommodate world data including the MiniBooNE and LSND excesses with a small number of free parameters. Evidence for sidereal variation in the MiniBooNE excesses would provide a distinctive direct signal of Lorentz violation.

3. Analysis

We use the SME formalism for the general search for Lorentz violation [21]. The SME is an effective quantum field theory and the minimum extension of the Standard Model including particle Lorentz and CPT violation [21]. A variety of data have been analyzed under this formalism [22], including neutrino oscillations [6–8]. In the SME formalism for neutrinos, the evolution of a neutrino can be described by an effective Hamiltonian [3],

$$\left(h_{\text{eff}}^\nu\right)_{ab} \sim \frac{1}{E}\left[(a_L)^\mu p_\mu - (c_L)^{\mu\nu} p_\mu p_\nu\right]_{ab}. \tag{1}$$

Here, E and p_μ are the energy and the four-momentum of a neutrino, and $(a_L)_{ab}^\mu$ and $(c_L)_{ab}^{\mu\nu}$ are CPT-odd and CPT-even SME coefficients in the flavor basis. Under the assumption that the baseline is short compared to the oscillation length [23], the $\nu_\mu \to \nu_e$ oscillation probability takes the form,

$$P \simeq \frac{L^2}{(\hbar c)^2}\Big|(\mathcal{C})_{e\mu} + (\mathcal{A}_s)_{e\mu}\sin\omega_\oplus T_\oplus + (\mathcal{A}_c)_{e\mu}\cos\omega_\oplus T_\oplus$$
$$+ (\mathcal{B}_s)_{e\mu}\sin 2\omega_\oplus T_\oplus + (\mathcal{B}_c)_{e\mu}\cos 2\omega_\oplus T_\oplus\Big|^2. \tag{2}$$

This probability is a function of sidereal time, $T_\oplus$. Four parameters $(\mathcal{A}_s)_{e\mu}$, $(\mathcal{A}_c)_{e\mu}$, $(\mathcal{B}_s)_{e\mu}$, and $(\mathcal{B}_c)_{e\mu}$ are sidereal time dependent, and $(\mathcal{C})_{e\mu}$ is a sidereal time-independent parameter. We use a baseline distance of $L = 522.6$ m, where the average pion decay length is subtracted from the distance between the neutrino production target and detector. And $\omega_\oplus$ is the sidereal time angular frequency described shortly. These parameters are expressed in terms of SME coefficients and directional factors [23]. The same formula describes the $\bar\nu_\mu \to \bar\nu_e$ oscillation probability by switching the signs of the CPT-odd SME coefficients. We neglect the standard neutrino mass term, $m_{e\mu}^2/E \ll 10^{-20}$ GeV, which is well below our sensitivity, discussed later.

For this analysis, we convert the standard GPS time stamp for each event to local solar time (period 86,400.0 s) and sidereal time (period 86,164.1 s). We then define the local solar time angular

[1] Present address: University of California, Riverside, CA 92521, USA.
[2] Postal address: Fermilab, MS309, PO Box 500, Batavia, IL 60510, USA.
[3] Deceased.
[4] Present address: IFIC, Universidad de Valencia and CSIC, Valencia 46071, Spain.
[5] Present address: Imperial College, London SW7 2AZ, United Kingdom.
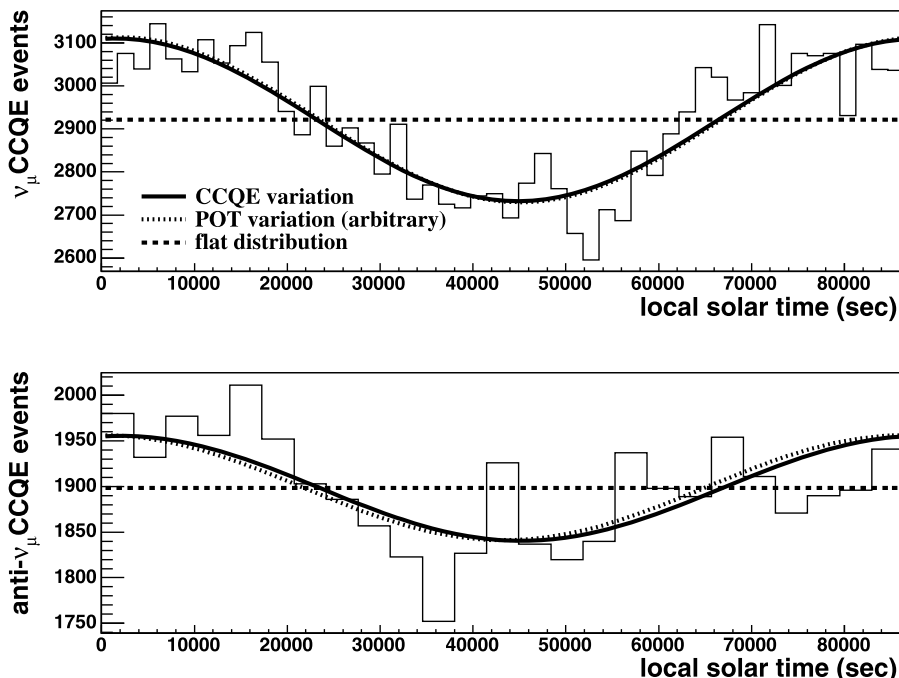
Fig. 1. The top (bottom) plot shows the ν_μCCQE ($\bar{\nu}_\mu$CCQE) local solar time distribution. The solid curves are fit functions extracted from the CCQE event distributions, and the dotted curves are from the POT distributions (arbitrary units) during the same period of data taking. The dashed line shows a flat distribution.

frequency $\omega_\odot = \frac{2\pi}{86,400.0}$ (rad/s) and the sidereal time angular frequency $\omega_\oplus = \frac{2\pi}{86,164.1}$ (rad/s). The time origin can be arbitrary, but we follow the standard convention with a Sun-centered coordinate system [6]. We choose a time-zero of 58 min after the autumnal equinox of 2002 (September 23, 04:55 GMT), so that this serves not only as the sidereal time-zero, but also as the solar time-zero since Fermilab is on the midnight point at this time. The local coordinates of the BNB are specified by three angles [23], colatitude $\chi = 48.2°$, polar angle $\theta = 89.8°$, and azimuthal angle $\phi = 180.0°$.

Any time-dependent background variations, such as the time variation of detector and BNB systematics, are important. To evaluate these, we use our high statistics CCQE samples (Fig. 1). These data are from our ν_μCCQE double-differential cross section measurement sample [24] composed of 146,070 events (5.58×10^{20} POT) and our $\bar{\nu}_\mu$CCQE candidate sample [25] composed of 47,466 events (5.66×10^{20} POT). The $\nu_\mu(\bar{\nu}_\mu)$CCQE local solar time distribution exhibits ±6(3)% variation.

The same variation in local solar time is observed in the POT for both neutrino and anti-neutrino mode data taking periods. Therefore, the POT variation is the dominant time-dependent systematic error. The amplitude is negligible in $\bar{\nu}_\mu$CCQE sidereal time distribution; however, it persists in ~3% variations in ν_μCCQE sidereal time distribution. We evaluate the impact of this variation on our analysis by correcting POT variation event by event in ν_e ($\bar{\nu}_e$) candidate data. It turns out the correction only has a negligible effect. Thus we decide to use unweighted events. This also simplifies the unbinned likelihood function used in later analysis. Figs. 2 and 3 show the ν_e and $\bar{\nu}_e$ oscillation candidates' sidereal time distributions both with and without the POT correction. These plots verify that time-dependent systematics are negligible in this analysis.

To check for a general deviation from a flat distribution (null sidereal variation hypothesis), we perform an unbinned K–S test [26] as a statistical null hypothesis test for both the ν_e and $\bar{\nu}_e$ samples. The K–S test is suitable in our case because it is sensitive to runs in distributions, which may be a characteristic feature

Table 1
A summary of K–S test results on the sidereal and local solar time distributions. The top table is for ν_e candidate data, and the bottom table is for $\bar{\nu}_e$ candidate data. The three rows show the average neutrino energy of each sample, number of events, and the K–S test compatibility with the null hypothesis. The test is performed in three energy regions, and for both local solar time and sidereal time distributions.

	Low energy		High energy		Combined	
	solar	sidereal	solar	sidereal	solar	sidereal
			Neutrino mode			
$\langle E_\nu \rangle$	0.36 GeV		0.82 GeV		0.71 GeV	
#evt	544		420		964	
P(KS)	0.42	0.13	0.81	0.64	0.64	0.14
			Anti-neutrino mode			
$\langle E_\nu \rangle$	0.34 GeV		0.78 GeV		0.60 GeV	
#evt	119		122		241	
P(KS)	0.62	0.15	0.79	0.39	0.69	0.08

of the sidereal time-dependent hypothesis. Table 1 gives the result. The K–S test is applied to the low-energy, high-energy, and combined regions, for both neutrino and anti-neutrino mode data. To investigate the time-dependent systematics, we also apply the K–S test to the local solar time distribution. The test shows none of the twelve samples has less than 5% compatibility (~2σ), which we chose as a benchmark prior to the analysis. Hence, all samples are compatible with the null sidereal variation hypothesis. Interestingly, the sidereal time distributions tend to show lower compatibility with a flat hypothesis, but not by a statistically significant amount. These results indicate that any sidereal variation extracted from our data, discussed below, is not expected to be statistically significant.

To fit the data with the sidereal time-dependent model, we use a generalized unbinned maximum likelihood method [27]. This method finds the best fit (BF) model parameters by fitting data with a log likelihood function, ℓ. It is suitable for our analysis because this method has the highest statistical power for a low statistics sample. In this method, the log likelihood function ℓ is
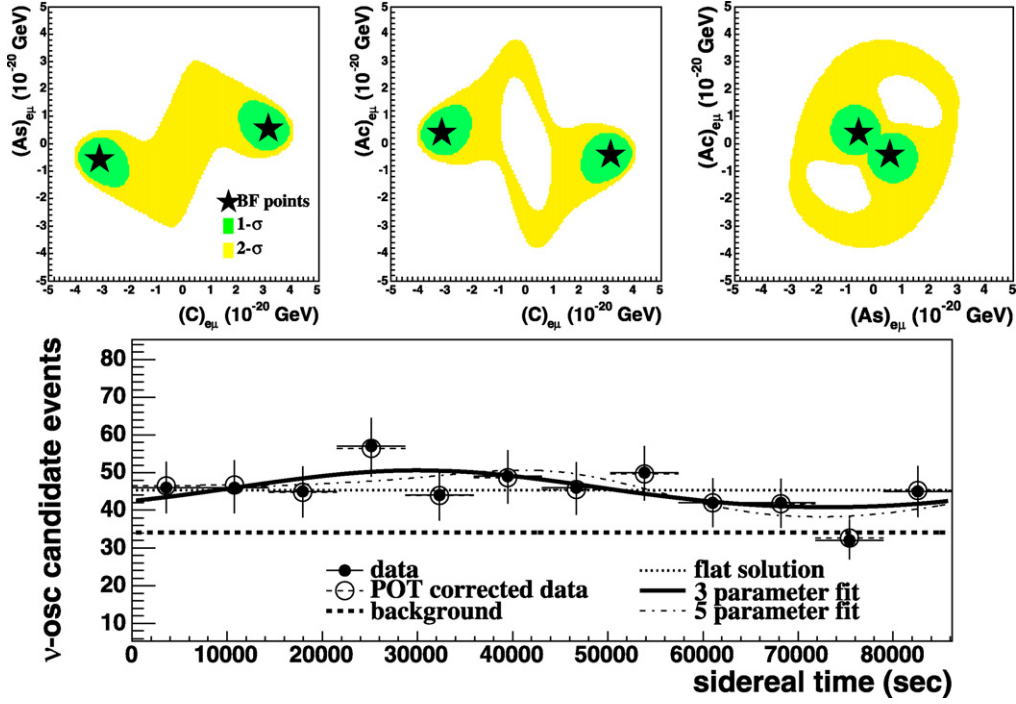
Fig. 2. (Color online.) Three-parameter fit results for the neutrino mode low-energy region. The top three plots show the projection of three-dimensional parameter space. The dark (light) shaded area shows the 1σ (2σ) contour in each projection. The stars show the BF points. The bottom plot shows the curves corresponding to the flat solution (dotted), three-parameter fit (solid), and five-parameter fit (dash-dotted), together with binned data (solid marker). The POT corrected data are also shown in open circle marker. Here, the fitted background is shown as a dashed line, and the BF value is 1.00 (*i.e.*, equivalent to the central value of the predicted background).
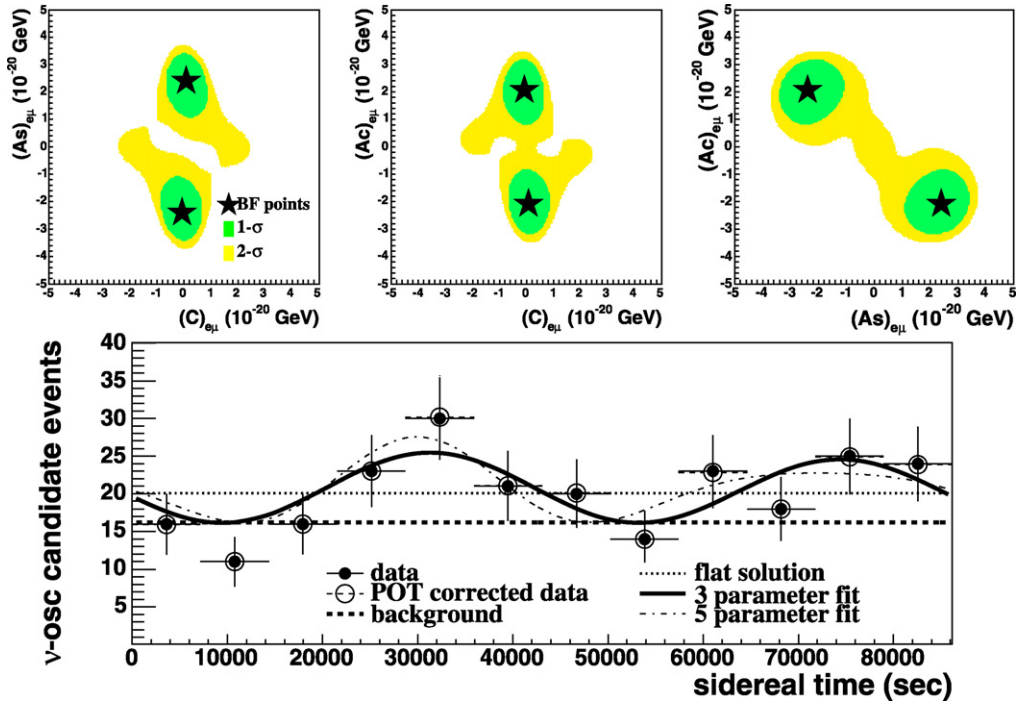

Fig. 3. Three-parameter fit results for the anti-neutrino mode combined region. Notations are the same as Fig. 2. Here, the BF value for the fitted background is 0.97 (3% lower than the central value of the predicted background).

constructed by adding ℓ_i from each event. After dropping all constants, ℓ_i has the following expression,

$$\ell_i = -\frac{1}{N}(\mu_s + \mu_b) + \ln\left[\mu_s \mathcal{F}_s^i + \mu_b \mathcal{F}_b^i\right] - \frac{1}{2N}\left(\frac{\mu_b - \bar{\mu}_b}{\sigma_b}\right)^2. \quad (3)$$

Here, N is the number of observed candidate events; μ_s is the predicted number of signal events, which is given by the time integral of Eq. (2) together with the estimated efficiency; μ_b is the predicted number of background events; $\mathcal{F}_s$ is the probability density function (PDF) for the signal and is a function of sidereal

Table 2
The fit parameters for the neutrino mode low-energy region and the anti-neutrino mode combined region. The BF points are the MLL points of the log likelihood function, in top rows from left to right: BF values, 1σ statistical errors, and 1σ systematic errors. The 2σ limits are also shown. Bottom rows show detailed expressions of each sidereal fit parameter in terms of SME parameters and directional factors [23]. The upper (lower) sign of $(a_L)^{\lambda}_{e\mu}$ terms is applied for neutrino (anti-neutrino) results, due to the CPT-odd nature. The average neutrino energy "$\langle E \rangle$" is 0.36 GeV for the neutrino mode low-energy region and 0.60 GeV for the anti-neutrino mode combined region (Table 1).

	ν-mode BF	2σ limit	$\bar{\nu}$-mode BF	2σ limit
$|(\mathcal{C})_{e\mu}|$	$3.1 \pm 0.6 \pm 0.9$	< 4.2	$0.1 \pm 0.8 \pm 0.1$	< 2.6
$|(\mathcal{A}_s)_{e\mu}|$	$0.6 \pm 0.9 \pm 0.3$	< 3.3	$2.4 \pm 1.3 \pm 0.5$	< 3.9
$|(\mathcal{A}_c)_{e\mu}|$	$0.4 \pm 0.9 \pm 0.4$	< 4.0	$2.1 \pm 1.2 \pm 0.4$	< 3.7
	SME coefficients combination (unit 10^{-20} GeV)			
$|(\mathcal{C})_{e\mu}|$	$\pm[(a_L)^{T}_{e\mu} + 0.75(a_L)^{Z}_{e\mu}] - \langle E \rangle[1.22(c_L)^{TT}_{e\mu} + 1.50(c_L)^{TZ}_{e\mu} + 0.34(c_L)^{ZZ}_{e\mu}]$			
$|(\mathcal{A}_s)_{e\mu}|$	$\pm[0.66(a_L)^{Y}_{e\mu}] - \langle E \rangle[1.33(c_L)^{TY}_{e\mu} + 0.99(c_L)^{YZ}_{e\mu}]$			
$|(\mathcal{A}_c)_{e\mu}|$	$\pm[0.66(a_L)^{X}_{e\mu}] - \langle E \rangle[1.33(c_L)^{TX}_{e\mu} + 0.99(c_L)^{XZ}_{e\mu}]$			

time and the fitting parameters (Eq. (2) with proper normalization); $\mathcal{F}_b$ is the PDF for the background; σ_b is the 1σ error on the predicted background; and $\bar{\mu}_b$ is the central value of the predicted total background events. Two sources contribute equally to the background: intrinsic beam background and mis-identification (mainly π°s). Their total variation is assigned as the systematic error, assumed to be time independent. Details can be found in [4,5].

The parameter space is scanned (grid search method) to find the largest ℓ, or the maximum log likelihood (MLL) point, and this MLL point provides the combination of the BF parameters. The log likelihood function includes six parameters, five that are functions of SME coefficients, and one for the background. However, the background term is constrained within a $\pm 1\sigma$ range. Neither the neutrino nor the anti-neutrino mode data allow us to extract errors if we fit all five parameters at once, due to the high correlation of parameters. Therefore, we set $(\mathcal{B}_s)_{e\mu}$ and $(\mathcal{B}_c)_{e\mu}$ to zero and concentrate on three parameters ($(\mathcal{C})_{e\mu}$, $(\mathcal{A}_s)_{e\mu}$, and $(\mathcal{A}_c)_{e\mu}$) for the uncertainty estimates. Since the five-parameter fit is quantitatively similar to the three-parameter fit, we will focus the discussion of the results on the three-parameter fits. This three-parameter fit also corresponds to the case with only CPT-odd SME coefficients [23].

4. Results

Fig. 2 shows the neutrino mode low-energy region fit results. The top three plots show the three projections of three-dimensional parameter space. Because of the square of fitting parameters in the PDF, the BF point has a sign ambiguity and is always duplicated. The 1σ and 2σ contours are formed from a constant slice of the log likelihood function in the three-dimensional parameter space. To avoid under coverage, these slices are expanded until they enclose 68% (1σ) or 95% (2σ) of BF points for the three-parameter fit of simulated, or "fake," data sets with the signal. Note that because fitting parameters are not linear in the PDF, twice the 1σ error does not yield the 2σ error.

A null sidereal variation hypothesis, or a flat solution, is equivalent to a three- or five-parameter fit solution where only the $(\mathcal{C})_{e\mu}$ parameter is nonzero. The fit to neutrino data favors a nonzero solution only for the $(\mathcal{C})_{e\mu}$ term. The bottom plot in Fig. 2 shows data plotted against curves corresponding to the flat solution and the best fits for three- and five-parameter functions. Since all three curves are close to each other, the solution of neutrino mode is dominated by the sidereal time-independent component. To find the significance of time dependence over the flat distribution, fake data sets without a signal are formed where the ν_e candidate

events are simulated without any time structure. The MLL difference between the three-parameter fit and the flat solution is used to form a $\Delta\chi^2$, and the expected $\Delta\chi^2$ distribution is determined by testing 500 random distributions from the fake data sets. This test shows that there is a 26.9% chance that a random distribution of ν_e candidate events would yield a $\Delta\chi^2$ value equal to, or greater than, the value observed for the data. This result is consistent with the sensitivity of this experiment. We estimate our sensitivity to the limited case. First, a 2σ threshold is set from this $\Delta\chi^2$ distribution. Then, time-dependent amplitudes were incrementally increased in the model until the 2σ threshold was exceeded. When we assume $(\mathcal{C})_{e\mu} \neq 0$ and $(\mathcal{A}_s)_{e\mu} = (\mathcal{A}_c)_{e\mu} \neq 0$, the 2σ discovery threshold of sidereal time-dependent amplitudes from $\nu_e(\bar{\nu}_e)$ candidate data statistics are $0.8(1.1)\times10^{-20}$ GeV.

Fig. 3 shows the analogous fit results for the anti-neutrino mode combined energy region. Due to lower statistics, the combined region is used rather than dividing the data into two subsets. Unlike the neutrino mode low-energy region, the $(\mathcal{C})_{e\mu}$ parameter no longer significantly deviates from zero. The fit to anti-neutrino data favors a nonzero solution for the $(\mathcal{A}_s)_{e\mu}$ and $(\mathcal{A}_c)_{e\mu}$ parameters at the nearly 2σ level. Performing the same $\Delta\chi^2$ test as is outlined above results in only 3.0% of the random distributions from the $\bar{\nu}_e$ candidate events having a $\Delta\chi^2$ value exceeding the value observed for the data. Note that this is consistent with the 8% compatibility with a flat hypothesis found with the K–S test (Table 1).

Table 2 shows fit parameters for the neutrino mode low-energy region and anti-neutrino mode combined region. All errors are estimated from 1σ contours of parameter space projections. Errors are asymmetric, but we choose the larger excursions as the symmetric errors for simplicity. The 2σ contours provide the limits. In principle, these fit parameters are complex numbers. Here, all parameters are assumed to be real.

A naive estimation from Table 2 indicates possible SME coefficients to satisfy the MiniBooNE data are of order 10^{-20} GeV (CPT-odd) and 10^{-20} to 10^{-19} (CPT-even). However, these SME coefficients are too small to produce a visible effect for LSND [6]. On the other hand, any SME coefficients extracted from LSND [6] predict too large of a signal for MiniBooNE. Therefore, a simple picture using Lorentz violation to explain both data sets leaves some tension, and a mechanism to cancel the Lorentz-violating effect at high energy [3,19,20] is needed.

The limit on each SME coefficient can be extracted from Table 2 by assuming all SME coefficients to be zero, except one. This process ignores correlations and somewhat ambiguous but is widely accepted in the community. In this way, our limits on

sidereal time-dependent SME coefficients ($(a_L)^X_{e\mu}$, $(a_L)^Y_{e\mu}$, $(c_L)^{TX}_{e\mu}$, $(c_L)^{TY}_{e\mu}$, $(c_L)^{XZ}_{e\mu}$, $(c_L)^{XZ}_{e\mu}$) are weaker than the MINOS near detector analysis [28]; however, we can set the first limits on sidereal time-independent coefficients ($(a_L)^T_{e\mu} < 4 \times 10^{-20}$ GeV, $(a_L)^Z_{e\mu} < 6 \times 10^{-20}$ GeV, $(c_L)^{TT}_{e\mu} < 1 \times 10^{-19}$, $(c_L)^{TZ}_{e\mu} < 8 \times 10^{-20}$, $(c_L)^{ZZ}_{e\mu} < 3 \times 10^{-19}$).

5. Summary

In summary, we performed a sidereal time variation analysis for MiniBooNE ν_e and $\bar{\nu}_e$ appearance candidate data. For the neutrino mode low-energy region, K–S test statistics indicate the null hypothesis is compatible at the 13% level, and the relative improvement in the likelihood between the null hypothesis and the three-parameter fit occurs 26.9% of the time in random distributions from a null hypothesis. Analysis of the combined energy region in anti-neutrino mode results in a K–S test that indicates an 8% compatibility with the null hypothesis; however, the relative improvement in the likelihood between the null hypothesis and the three-parameter fit only occurs 3.0% of the time in random distributions from a null hypothesis. The limits of fit parameters, 10^{-20} GeV, are consistent with Planck-scale suppressed physics. This is the first sidereal variation test for an anti-neutrino beam of $\sim$1 GeV energy and $\sim$500 m base line. These limits are currently the best limits on the sidereal time-independent $(a_L)_{e\mu}$ and $(c_L)_{e\mu}$ SME coefficients. These limits can be significantly improved by long baseline ν_e ($\bar{\nu}_e$) appearance experiments, such as T2K [29] and NOvA [30].

Acknowledgements

References

[1] V.A. Kostelecký, S. Samuel, Phys. Rev. D 39 (1989) 683.
[2] S. Coleman, S.L. Glashow, Phys. Rev. D 59 (1999) 116008.
[3] V.A. Kostelecký, M. Mewes, Phys. Rev. D 69 (2004) 016005.
[4] A.A. Aguilar-Arevalo, et al., Phys. Rev. Lett. 98 (2007) 231801;
    A.A. Aguilar-Arevalo, et al., Phys. Rev. Lett. 102 (2009) 101802.
[5] A.A. Aguilar-Arevalo, et al., Phys. Rev. Lett. 103 (2009) 111801;
    A.A. Aguilar-Arevalo, et al., Phys. Rev. Lett. 105 (2010) 181801.
[6] L.B. Auerbach, et al., Phys. Rev. D 72 (2005) 076004.
[7] P. Adamson, et al., Phys. Rev. Lett. 101 (2008) 151601;
    P. Adamson, et al., Phys. Rev. Lett. 105 (2010) 151601.
[8] R. Abbasi, et al., Phys. Rev. D 82 (2010) 112003.
[9] V.A. Kostelecký, M. Mewes, Phys. Rev. D 70 (2004) 031902(R).
[10] A.A. Aguilar-Arevalo, et al., Phys. Rev. D 79 (2009) 072002.
[11] A.A. Aguilar-Arevalo, et al., Nucl. Instrum. Meth. A 599 (2009) 28.
[12] R.B. Patterson, et al., Nucl. Instrum. Meth. A 608 (2009) 206.
[13] A.A. Aguilar-Arevalo, et al., Phys. Rev. Lett. 100 (2008) 032301.
[14] http://www-boone.fnal.gov/for_physicists/data_release/lowe.
[15] http://www-boone.fnal.gov/for_physicists/data_release/nuebar2010.
[16] A. Aguilar-Arevalo, et al., Phys. Rev. D 64 (2001) 112007.
[17] J. Kopp, et al., Phys. Rev. Lett. 107 (2011) 091801.
[18] O.W. Greenberg, Phys. Rev. Lett. 89 (2002) 231602.
[19] T. Katori, V.A. Kostelecký, R. Tayloe, Phys. Rev. D 74 (2006) 105009.
[20] J.S. Díaz, V.A. Kostelecký, Phys. Lett. B 700 (2011) 25;
    J.S. Díaz, V.A. Kostelecký, Phys. Rev. D 85 (2012) 016013.
[21] D. Colladay, V.A. Kostelecký, Phys. Rev. D 55 (1997) 6760;
    D. Colladay, V.A. Kostelecký, Phys. Rev. D 58 (1998) 116002;
    V.A. Kostelecký, Phys. Rev. D 69 (2004) 105009.
[22] For recent reviews see, for example, V.A. Kostelecký (Ed.), CPT and Lorentz Symmetry V, World Scientific, Singapore, 2011;
    V.A. Kostelecký, N. Russell, Rev. Mod. Phys. 83 (2011) 11.
[23] V.A. Kostelecký, M. Mewes, Phys. Rev. D 70 (2004) 076002.
[24] A.A. Aguilar-Arevalo, et al., Phys. Rev. D 81 (2010) 092005.
[25] A.A. Aguilar-Arevalo, et al., Phys. Rev. D 84 (2011) 072005.
[26] W.H. Press, et al., Numerical Recipes in C++: The Art of Scientific Computing, Cambridge University Press, New York, 2002.
[27] L. Lyons, Statistics for Nuclear and Particle Physicists, Cambridge University Press, New York, 1989.
[28] P. Adamson, et al., Phys. Rev. D 85 (2012) 031101(R).
[29] K. Abe, et al., Phys. Rev. Lett. 107 (2011) 041801.
[30] D.S. Ayres, et al., arXiv:hep-ex/0503053.